Chemical Engineering Journal 225 (2013) 423–432

Contents lists available at SciVerse ScienceDirect

Chemical Engineering Journal

journal homepage: www.elsevier.com/locate/cej

A kinetic model for the degradation of dichloroacetic acid and formic acid in water employing the H_2O_2/UV process

Melisa L. Mariani, Rodolfo J. Brandi, Alberto E. Cassano, Cristina S. Zalazar *

INTEC (Universidad Nacional del Litoral and CONICET), Güemes 3450, 3000 Santa Fe, Argentina

HIGHLIGHTS

- This work reports the degradation kinetics of a mixture of pollutants in water.
- The model is based on a complete reaction mechanism using H_2O_2/UV radiation.
- The model describes the effect of the local irradiation rate.
- The model is experimentally validated.

ARTICLE INFO

Article history:
Received 14 August 2012
Received in revised form 24 March 2013
Accepted 26 March 2013
Available online 6 April 2013

Keywords:
Kinetics
UV/H_2O_2 process
Mixture of dichloroacetic and formic acids

ABSTRACT

A kinetic model for the simultaneous degradation of dichloroacetic acid (DCAA) and formic acid (FA) has been developed. The oxidation is produced by the combination of hydrogen peroxide (HP) and UV (253.7 nm) radiation. A set of four equations, three differentials and one algebraic, represents the time evolution of the concentration of DCAA, FA, HP and hydrochloric acid (HCl), a measurable by-product. The model is based on a complete reaction mechanism, which comprises hydrogen peroxide photolysis and decomposition of dichloroacetic and formic acids. It takes into account the effect of non-uniform distribution of the local rate of absorbed photons. The mathematical model renders simulation results that agree with the experimental data. It was also shown that FA decays much faster than DCAA.

1. Introduction

Advanced oxidation process (AOP) has been the topic of numerous research works in the last decades [1–3]. These processes include technologies such as O_3/H_2O_2, O_3/UV, H_2O_2/UV, O_3/H_2O_2/UV, Fe^{2+}/H_2O_2, Fe^{2+}/H_2O_2/UV, TiO_2/UV, etc., just to mention some of the most widely used. AOPs involve the generation and subsequent reaction of very reactive, intermediate species, such as the hydroxyl radical (·OH) that oxidizes many organic and inorganic compounds due to its high oxidation potential (SOP = 2.8 V).

Even though conventional technologies that transfer the pollutant from one phase to another, such as adsorption or gas stripping, are still widely accepted in the market, AOPs research has set as a very important target to make these technologies more attractive because they can achieve a reasonable yield for removing some selected contaminants instead of transferring the pollution from one place to another. AOPs are also efficient processes for removing non-biodegradable and refractory organic compounds.

The UV/H_2O_2 process has some qualities with respect to others AOPs. Hydrogen peroxide (HP) is easier to transport, store and operate; also it is also highly soluble in water; the equipment and processing costs are not high; and it has shown efficiency for degrading several pollutants such as pesticides [4], methyl tert-butyl ether (MTBE) [5], phenols [6] and dyes [7,8]. Considering these advantages, this method seems to be an appealing alternative.

Designing a low cost UV/H_2O_2 process for commercial applications requires the determination of the effects of important design and operational variables. With this purpose, a representative kinetic model should be able to describe the fate of the pollutants within the photoreactor regardless its shape and its relative configuration with respect to the irradiation system. In order to be effective, it requires the precise knowledge of the degradation pathways and the reaction rates constants corresponding to the interaction of hydroxyl radicals with the involved pollutants, and also of the photonic absorption rate effects on the reaction rates [9,10].

Kinetic models have been previously proposed by several research groups for predicting the decomposition rate of specific organic compound employing the UV/H_2O_2 technology in aqueous phase. The kinetic models for the UV/H_2O_2 process proposed by Lay [11] and Glaze et al. [12] considered most of the important reactions occurring in the reactor and were verified through experimental studies. The model was able to predict the concentration of a

* Corresponding author. Tel.: +54 (0)342 4511546; fax: +54 (0)342 4511087.
E-mail address: szalazar@santafe-conicet.gov.ar (C.S. Zalazar).

1385-8947/$ - see front matter © 2013 Elsevier B.V. All rights reserved.
http://dx.doi.org/10.1016/j.cej.2013.03.098

Nomenclature

C	concentration, mole L^{-1} (M)
e^a	local volumetric rate of photon absorption, Einstein $cm^{-3}\ s^{-1}$
G	incident radiation, Einstein $s^{-1}\ cm^{-2}$
k	kinetic constant, units depend on the reaction step
L	length, cm
HP	hydrogen peroxide
R	reaction rate, mole $L^{-1}\ s^{-1}$
r'	molar concentration ratio
t	time, s
V	volume, cm^3
x	rectangular Cartesian coordinate, cm
Q	flow rate, L min^{-1}

Greek letters

α	molar naperian absorptivity, $cm^2\ mole^{-1}$ or parameter k_8/k_2
β	parameter
κ	volumetric absorption coefficient, cm^{-1}
λ	wavelength, nm

Subscripts

DCAA	relative to dichloroacetic acid
FA	relative to formic acid
FA_H	relative to formic acid protonated
FA_A	relative to ionized formic acid
Hom	relative to homogeneous phase
i	relative to species i
HP	relative to hydrogen peroxide
R	denotes reactor volume
T	denotes total reaction volume
t	time, s
w	relative to the wall
λ	relative to monochromatic radiation of wavelength λ
MAX	relative to maximum

Superscripts

0	relative to an initial condition

Special symbols

$\langle\rangle$	average value over a defined space

pollutant (1,2-dibromo-3-chloropropane) as a function of time at different hydrogen peroxide concentrations. Liao and Gurol [13] developed a kinetic model for *n*-chlorobutane which considers the influence of background organic matter on the reactor performance. In the model developed by Stefan et al. [14], the kinetic degradation pathways for the breakdown of acetone were proposed, and the degradation of acetone and by-products were examined. Crittenden et al. [15] developed a dynamic kinetic model using the UV/H_2O_2 process in a completely mixed batch reactor. The model included the photochemical initiation and other elementary chemical and photochemical reactions. The model does not assume that the net formation rate of free radical species is zero, which would mean that the rate of their formation equals the rate of their consumption (the pseudo-steady state assumption). The model was tested by predicting the destruction of a probe compound (1,2-dibromo-3-chloropropane) in distilled water with the addition of carbonate and bicarbonate ions. Song et al. [16] proposed a kinetic model for predicting the decomposition of alachlor in the presence of natural organic matter and other free-radical scavengers under different water quality and operating conditions. In the work developed by Kusic et al. [17], the goal was to develop a mathematical model for predicting the degradation of an azo dye model pollutant by three photooxidation processes: UV/H_2O_2, $UV/S_2O_8^{2-}$ and UV/O_3. The model predicted the conversion of azo dye and the formation and subsequent degradation of the main intermediates and the final inorganic products of the pollutant mineralization.

In the current work, the development of kinetic expressions to represent the photodegradation rates of a mixture of two compounds in water employing the UV/H_2O_2 process is proposed. The model compounds were dichloroacetic acid (DCAA), a typical by-product of chlorine disinfection, and formic acid (FA). Both of them were used at the same level of concentration throughout the experiments. The kinetic model is based on a complete reaction scheme developed in a previous work [18] and includes the rigorous modeling of the effects produced by the spatial distribution of the existing radiation field on the reaction rate. The evaluation of the photon absorption rate inside the reactor was achieved by solving the radiative transfer equation (RTE) for the homogeneous system because this effect is not uniform and depends on the local distribution of the spectral radiance, afterwards, must be subjected to a reactor volume averaging integral.

However, an additional important aim of this work is to verify to what extent it is possible to use the intrinsic kinetics of the decomposition of two organic compounds to model the decomposition of the mixture of both, using the mechanism obtained separately for each one of them.

The idea is to widen the methodology to increasingly complex systems and to determine the limitations that may appear in real water applications that would force to resort to new procedures to solve the difficulties that could have been found.

2. Materials and methods

2.1. Chemicals

The following reactants were used: (a) DCAA (Merck, p.a., >98%) (b) FA (Merck, 98–100%), (c) H_2O_2 (Ciccarelli p.a., 30% p/v), (d) KCl (Merck, p.a., >99%) and (e) catalase from bovine liver (Fluka, >2000 units mg^{-1}) (1 Unit of the employed reagent corresponds

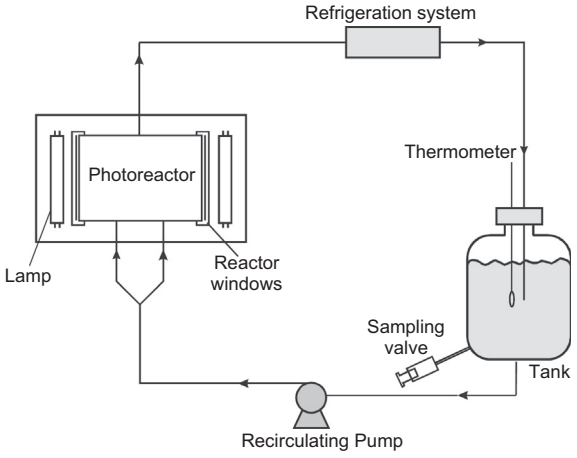

Fig. 1. Experimental setup.

Table 1
Experimental conditions.

Variable	Value
DCAA initial concentration	1.6×10^{-4} to 3.9×10^{-4} (M) (20–50 mg L^{-1})
FA initial concentration	4.3×10^{-4} to 10.9×10^{-4} (M) (20–50 mg L^{-1})
HP initial concentration	0–3.2×10^{-2} (M) (0–1100 mg L^{-1})
Incident radiation	
Heraeus UV–C 40 W	23.3 (Einstein cm^{-2} s^{-1}) $\times 10^9$
Philips TUV 15 W	10.4 (Einstein cm^{-2} s^{-1}) $\times 10^9$
Reaction time	18.000 s (5 h)
Temperature	20 (°C)
Initial pH	3.5

to the amount of enzyme that decomposes 1 μmol min^{-1} of H_2O_2 at pH = 7 and 25 °C). Deionized water was used for all experiments.

2.2. Experimental reactor and operating conditions

The study was carried out in a batch photoreactor operated inside a closed recycling loop (Fig. 1). The reactor was a cylinder with two parallel flat windows made of Suprasil quartz. Radiation was produced with two low-pressure mercury vapor lamps (λ = 253.7 nm). Each window permitted the interposing of one shutter to block the passage of light when necessary. The photoreactor's volume (V_R) was 110 cm^3 and the total volume (V_T) of the system was 2000 cm^3. The reagents and products in the recirculated water enter the reactor through two inlet ports located at the reactor wall which allow a tangential, powerful flow to the interior of the reaction zone. The water exits the reactor through an outlet port located on the opposite side to that where the inlets are located. This design allows collisions of the fluid with the reactor walls and sudden changes of directions in the reactor volume. The internal diameter of the entry and exit pipes of the reactor is 1 cm. The reacting solution flow rate (3 L min^{-1}) originates a Reynolds number (Re) = 3180 in each of the two supply tubes and a Re = 6370 in the exit tube. This operation system generates a strong turbulence in the reactor volume, which ensures an excellent mixing. In the case of the tank, the mixture is additionally improved by the existence of a magnetic stirring system that operates with a Teflon rod of 5 cm long at a speed of 1500 rpm. More considerations concerning mixing in the reactor will be made in the section corresponding to the analysis of the results. A detailed description of the photoreactor has been presented elsewhere [19].

The experimental conditions used in this study were the same as those used in a previous work on the experimental degradation of the mixture DCAA and FA in water using the UV/H_2O_2 process [18]. Hence, experiments were carried out in the following range of the significant experimental variables: (1) DCAA initial concentration between 1.6×10^{-4} and 3.9×10^{-4} M and FA initial concentration between 4.3×10^{-4} and 10.9×10^{-4} M; (2) H_2O_2 initial concentration between 0 and 3.2×10^{-2} M; (3) Incident radiation rates produced by tubular germicidal lamps with different output irradiance between 10.4×10^{-9} and 23.3×10^{-9} Einstein cm^{-2} s^{-1} (measured with potassium ferrioxalate actinometry [20] and calculated according to [21]). The initial pH was 3.5 and this value was obtained from the mixture of DCAA and FA in the working solution. The pH remained almost constant during the reaction. The experimental conditions are shown in Table 1.

2.3. Degradation procedure

In each experiment a working solution (2000 cm^3) of DCAA, FA and HP was prepared using deionized water. The photoreactor was filled with the solution and then recirculation was set. During each run, samples of 25 ml were taken inside clean vials every 60 min. Once each run had finished, the photoreactor was carefully washed three times with tap water and twice with deionized water.

2.4. Analytical methods

DCAA, FA and chloride ion were analyzed by ion chromatograph with a suppressed conductivity detector (Waters 432) employing an Ion Pac AS4A-SC (4 × 250 mm) analytical column. The injection volume was 20 μl. The flow rate of the mobile phase, $NaHCO_3$ (1.7 mM)/Na_2CO_3 (1.8 mM), was fixed at 1 ml min^{-1}. Duplicate injections of each sample were made. Prior to the liquid chromatograph injection, a fixed volume 350 μl of catalase solution (170 mg L^{-1}) was added to each sample. HP was analyzed with spectrophotometric methods at 350 nm according to Allen et al. [22] employing a Cary 100 Bio (Varian) UV–visible instrument. Total organic carbon (TOC) was measure with Shimadzu TOC-5000A analyzer. The precision of the TOC measurements were in the range of ±1 mg of organic carbon L^{-1}. pH was monitored with a HI 98127 Hanna pHmeter (accuracy: ±0.1).

3. Modeling aproach

3.1. Mass balance

The mass balance was solved in order to obtain the theoretical evolution of DCAA, FA and HP. For this purpose, a number of well-grounded assumptions were made: (i) there is a differential conversion per pass in the reactor (to be supported with results analyzed further ahead); (ii) the system is perfectly mixed (same observation as above); (iii) direct photolysis is neglected, as shown in a previous work [18]; and (iv) the recirculation flow rate is high (3 L min^{-1}). These operating conditions greatly simplify the mathematical analysis of the experimental data of the recycling system [23]. If assumptions (i and ii) are not fulfilled, the mass balance becomes much more difficult. These assumptions can be easily fulfilled if condition (iv) is satisfied and the reaction rate is relatively slow. Conversely, when the listed assumptions are satisfied, they permit the rigorous application of an ordinary differential equation as simple as Eq. (1) below. Under the previous operating conditions, changes in concentration in the tank are related to the reaction rates according to Eq. (1) [24].

$$\left.\frac{dC_i(t)}{dt}\right|_{Tank} = \frac{V_R}{V_T}\left\langle R_{Hom,i_i}(x,t)\right\rangle_{V_R} \quad (1)$$

with the initial condition that $\langle C_i(x,0)\rangle_{V_R} = C_i^0$.

where C_i is the concentration of DCAA, FA or HP, $R_{Hom,i}$ is the homogeneous reaction rate corresponding to DCAA, FA and HP. Note that the reaction rate is preceded by the ratio of the photoreactor volume (V_R) over the total volume (V_T). Hence, this ratio results from the special type of batch reactor (a recycle with a tank) that is employed in this work.

3.2. Kinetic model

3.2.1. Reaction scheme and kinetic equations

The reaction path for the degradation of DCAA and FA with H_2O_2/UV is illustrated in Table 2.

The main interactions between H_2O_2 with UV radiation and free radicals are well represented by reactions (1)–(7) and its kinetic constants are well known [25–28]. Reactions (8)–(11) were taken from [24,32]. DCAA p*K*a is 1.26. Thus, at pH 3.5 used in this work DCAA exist essentially in its deprotonated form (Step 8).

Table 2
Reaction scheme.

No.	Steps	Reactions	Constants ($M^{-1}\ s^{-1}$)
(1)	Initiation	$H_2O_2 \xrightarrow{\Phi_{HP}} 2{\cdot}OH$	$\Phi_{HP} = 0.5$ (mol Einstein^{-1})
(2)	Propagation	$H_2O_2 + {\cdot}OH \xrightarrow{k_2} HO_2^{\cdot} + H_2O$	$\mathbf{2.7 \times 10^7}$ (i)
(3)		$H_2O_2 + HO_2^{\cdot} \xrightarrow{k_3} {\cdot}OH + H_2O + O_2$	3.0 (ii)
(4)	Termination	$2{\cdot}OH \xrightarrow{k_4} H_2O_2$	5.5×10^9 (iii)
(5)		$2HO_2^{\cdot} \xrightarrow{k_5} H_2O_2 + O_2$	8.3×10^5 (iv)
(6)		${\cdot}OH + HO_2^{\cdot} \xrightarrow{k_6} H_2O + O_2$	6.6×10^9 (v)
(7)		${\cdot}OH + O_2^{\cdot-} \xrightarrow{k_7} OH^- + O_2$	7.0×10^{12} (vi)
(8)	Descomposition DCAA	$CCl_2\ HCOO^- + {\cdot}OH \xrightarrow{k_8} {\cdot}CCl_2\ COO^- + H_2O$	$\mathbf{5.8 \times 10^7}$ (vii) $\mathbf{9.2 \times 10^7}$ (viii)
(9)		${\cdot}CCl_2COO^- + O_2 \xrightarrow{k_9} {\cdot}OOCCl_2\ COO^-$	Rate approach the diffusion-controlled limits
(10)		$2{\cdot}OOCCl_2COO^- \xrightarrow{k_{10}} 2COCl_2 + 2CO_2 + O_2$	–
(11)		$COCl_2 + H_2O \xrightarrow{k_{11}} CO_2 + 2HCl$	9 s^{-1} (ix)
(12)	FA	$HCOOH + {\cdot}OH \xrightarrow{k_{12}} {\cdot}CO_2^- + H^+ + H_2O$	$\mathbf{1.3 \times 10^8}$ (x)
(13)		$HCOO^- + {\cdot}OH \xrightarrow{k_{13}} {\cdot}CO_2^- + H_2\ O$	$\mathbf{3.2 \times 10^9}$ (xi)
(14)		${\cdot}CO_2^- + O_2 \xrightarrow{k_{14}} CO_2 + O_2^-$	2.0×10^9 (xii)
(15)		$HCOOH \xrightarrow{K_{15}} HCOO^- + H^+$	1.77×10^{-4} (M)

(i, iii and iv) Taken from [25]; (ii) taken from [26]; (v) taken from [27]; (vi) taken from [28] (vii) taken from: [24]; (viii) taken from:[29]; (ix) taken from [30]; (x) and (xi) taken from [25]; (xii) taken from [31].

Since the p*K*a of FA is 3.75, at the working pH (3.5) the protonated and the ionized form of FA coexist. Step (12) corresponds to the reaction of the ·OH radical with the protonated formic acid (FA_H) and step (13) corresponds to the reaction of the ·OH radical with the ionized form of formic acid (FA_A). These steps have been proposed taking into account the reported reaction steps for the degradation of FA employing others AOPs like TiO_2/UV or H_2O_2/vacuum UV photoreactions [33–35]. Step (15) represents the equilibrium reaction for FA.

The reaction kinetics was formulated in terms of the mass action law for all the necessary reaction steps proposed in Table 2. Zalazar et al. [24] has shown that step 2 is the predominant propagation step and step 5 is the prevailing termination step. These results are in agreement with previous remarks published by [13]. Taking into account these reliable approximations, neglecting reactions (3), (4), and (6), a simplified kinetic scheme can be developed.

For DCAA:

$$R_{DCAA} = -k_8 C_{DCAA} C_{\cdot OH} \tag{2}$$

For FA_H and FA_A:

$$R_{FA_H} = -k_{12} C_{FA_H} C_{\cdot OH} \tag{3}$$

$$R_{FA_A} = -k_{13} C_{FA_A} C_{\cdot OH} \tag{4}$$

Therefore the global reaction rate for FA is:

$$R_{FA} = -k_{12} C_{FA_H} C_{\cdot OH} - k_{13} C_{FA_A} C_{\cdot OH} \tag{5}$$

The total concentration of FA in the mixture is calculated according to:

$$C_{FA} = C_{FA_H} + C_{FA_A} \tag{6}$$

From the equilibrium reaction constant (step 15):

$$K_{15} = \frac{C_{H^+} C_{FA_A}}{C_{FA_H}} \tag{7}$$

Therefore taking into account that the pH remains almost constant it is possible to relate the FA_A concentration with FA_H concentrations using Eq. (7):

$$C_{FA_A} = \left(\frac{K_{15}}{C_{H^+}}\right) C_{FA_H} = \omega C_{FA_H} \tag{8}$$

Finally it is possible to write the concentrations of FA_H and FA_A as a function of the total formic acid concentration (FA) as follows:

$$C_{FA_H} = \frac{1}{(1+\omega)} C_{FA} \tag{9}$$

$$C_{FA_A} = \frac{\omega}{(1+\omega)} C_{FA} \tag{10}$$

Finally, Eq. (5) can be written:

$$R_{FA} = -\left(\frac{k_{12} + \omega k_{13}}{1+\omega}\right) C_{FA} C_{\cdot OH} \tag{11}$$

For HP:

$$R_{HP} = -\Phi_{HP} e_\lambda^a - k_2 C_{HP} C_{\cdot OH} + k_5 C_{HO_2^{\cdot}}^2 \tag{12}$$

For unstable species ·OH $HO_2^{\cdot}$ and ${\cdot}CO_2^-$ resorting to the micro-steady-state approximation (MSSA):

$$R_{\cdot OH} = 2\Phi_{HP} e_\lambda^a - k_2 C_{HP} C_{\cdot OH} - k_8 C_{DCAA} C_{\cdot OH} - \left(\frac{k_{12} + \omega k_{13}}{1+\omega}\right) C_{FA} C_{\cdot OH} \cong 0 \tag{13}$$

$$R_{HO_2^{\cdot}} = k_2 C_{HP} C_{\cdot OH} - 2k_5 C_{HO_2^{\cdot}}^2 \tag{14}$$

$$R_{\cdot CO_2^-} = k_{13} C_{FA_A} C_{\cdot OH} - k_{14} C_{\cdot CO_2^-} C_{O_2} \cong 0 \tag{15}$$

$$R_{O_2^{\cdot-}} = k_{14} C_{\cdot CO_2^-} C_{O_2} - k_7 C_{\cdot OH} C_{O_2^{\cdot-}} \cong 0 \tag{16}$$

From Eq. (14):

$$C_{HO_2^{\cdot}}^2 = \frac{k_2 C_{HP} C_{\cdot OH}}{2k_5} \tag{17}$$

And resorting to Eq. (13):

$$C_{\cdot OH} = \left(\frac{2\Phi_{HP} e^{a}_{\lambda}}{k_2 C_{HP} + k_8 C_{DCAA} + \left(\frac{k_{12}+\omega k_{13}}{1+\omega}\right) C_{FA}} \right) \quad (18)$$

The reactions rates result:

$$R_{DCAA} = -k_8 C_{DCAA} \left[\frac{2\Phi_{HP} e^{a}_{\lambda}}{k_2 C_{HP} + k_8 C_{DCAA} + \left(\frac{k_{12}+\omega k_{13}}{1+\omega}\right) C_{FA}} \right] \quad (19)$$

$$R_{FA} = -\left[\frac{2\Phi_{HP} e^{a}_{\lambda}}{k_2 C_{HP} + k_8 C_{DCAA} + \left(\frac{k_{12}+\omega k_{13}}{1+\omega}\right) C_{FA}} \right] \times \left(\frac{k_{12} + \omega k_{13}}{1+\omega} \right) C_{FA} \quad (20)$$

$$R_{HP} = -\Phi_{HP} e^{a}_{\lambda} \left[1 + \frac{k_2 C_{HP}}{k_2 C_{HP} + k_8 C_{DCAA} + \left(\frac{k_{12}+\omega k_{13}}{1+\omega}\right) C_{FA}} \right] \quad (21)$$

In previous equations R represents molar reactions rates for DCAA, FA and HP respectively.Where $C_{DCAA} = C_{DCAA}(t)$ $C_{FA} = C_{FA}(t)$ and $C_{HP} = C_{HP}(t)$ are the molar concentrations of DCAA, FA and HP respectively. Φ_{HP} is the primary quantum yield and $e^{a}_{\lambda}(x,t)$ is the local volumetric rate of photon absorption (LVRPA) by H_2O_2. If we define $r_1 = (C_{DCAA})/(C_{HP})$ and $r_2 = (C_{FA})/(C_{HP})$ as well as the parameters $\alpha = (k_8)/(k_2)$ and $\beta = (k_{12} + \omega k_{13})((1+\omega)k_2)$, rearranging Eqs. (19)–(21) we finally get:

$$R_{DCAA} = -\alpha r_1 \left[\frac{2\Phi_{HP} e^{a}_{\lambda}}{1 + r_1\alpha + r_2\beta} \right] \quad (22)$$

$$R_{FA} = -\beta r_2 \left[\frac{2\Phi_{HP} e^{a}_{\lambda}}{1 + r_1\alpha + r_2\beta} \right] \quad (23)$$

$$R_{HP} = -\Phi_{HP} e^{a}_{\lambda} \left[1 + \frac{1}{1 + r_1\alpha + r_2\beta} \right] \quad (24)$$

In Table 2 the rate constants finally used in the proposed kinetic model are written in bold face characters (values of k_2, k_8, k_{12}, k_{13}). The parameters α and β were calculated from these reaction rate constants provided from references [24,25,29]. Since there are two values published for constant k_8, in Section 4.2 Model evaluation for DCAA and FA separately" this difference is discussed and an explanation is given for the choice of the value adopted in the kinetic model. The quantum yield (Φ_{HP}) was taken from the existing information [36,37]. The photon absorption effects were calculated by solving the radiation balance in the experimental reactor as shown below.

3.2.2. The HCl formation

For complete mineralization, each mole of DCAA that is decomposed should produce two moles of Cl^-. In a previous work [18], it was shown that this reaction does not have stable intermediates in aqueous media because $COCl_2$ is instantaneously hydrolyzed. In this mixture, only DCAA generates chloride ions and the stoichiometric relationship between them is clear. Therefore, the following algebraic equation must be always satisfied:

$$R_{HCl} = -2R_{DCAA} \quad (25)$$

Hence, the reaction rate of hydrochloric acid appearance is equal to twice the value of the reaction rate of DCAA disappearance.

3.3. The radiation balance

The radiation intensity effect was calculated by solving the radiation balance in the experimental reactor. The same configuration reactor was used in a previous work and the expression employed to compute the averaged LVRPA in the reactor volume was derived in [24]:

$$\left\langle e^{a}_{HP,\lambda}(x,t) \right\rangle_{V_R} = \frac{2G_{W,\lambda}}{L_R} \{1 - \exp[-\kappa_{HP,\lambda}(t) L_R]\} \quad (26)$$

where G_W is the incident radiation at the reactor wall and $\kappa_{\lambda,HP}$ is the linear naperian absorption coefficient of the reactant absorbing species.

The incident radiation G_W at $x = 0$ and $x = L_R$ was evaluated with actinometer measurements using potassium ferrioxalate [20] and the method described by Zalazar et al. [21].

3.4. Final equations

Volume averaging the reaction rates for the stable species DCAA, FA and HP Eqs. (22)–(24), and, if the cross sectional area of the reactor is constant, for a one-dimensional model, it is only necessary to perform the integral over the reactor length L_R:

$$\langle R_i(x,t) \rangle_{V_R} = \frac{1}{L_R} \int_{L_R} R_{i(x,t)dx} \quad (27)$$

Substituting Eq. (27) in each reaction's rate Eqs. (22)–(24), considering that according to the well mixed assumption all species concentrations are not a function of position and taking into account Eq. (1):

$$\frac{dC_{DCAA}(t)}{dt} = -\left(\frac{V_R}{V_T}\right) \alpha r_1 \left[\frac{2\Phi_{HP} \langle e^{a}_{HP,\lambda} \rangle}{1 + r_1\alpha + r_2\beta} \right] \quad (28)$$

$$\frac{dC_{FA}(t)}{dt} = -\left(\frac{V_R}{V_T}\right) \beta r_2 \left[\frac{2\Phi_{HP} \langle e^{a}_{HP,\lambda} \rangle}{1 + r_1\alpha + r_2\beta} \right] \quad (29)$$

$$\frac{dC_{HP}(t)}{dt} = \left(\frac{V_R}{V_T}\right) \left\{ -\Phi_{HP} \langle e^{a}_{HP,\lambda} \rangle \left[1 + \frac{1}{1 + r_1\alpha + r_2\beta} \right] \right\} \quad (30)$$

Eqs. (28)–(30) constitute one system of ordinary differential equations that was solved by the Runge–Kutta method.

4. Results and discussion

4.1. The intrinsic values of the obtained results

In addition to the precautions taken to use a rigorous modeling method, the kinetic rate equations obtained will be intrinsic if Eq. (1) is valid and if the experimental data were obtained under the chemical kinetic controlling regime.

With the object of establishing if the reactor operates in a differential manner and under conditions where there are no mass transport restrictions, one can resort to the one experimental run where the largest conversion in the shortest reaction time was obtained; i.e., (i) for FA, that is the compound that degrades faster [18], (ii) operating with the maximum incident radiation and (iii) working with the optimal ratio previously found [18].

With this information, it is possible to proceed to calculate the Damkolher number (Da). Since the concentration of HP is not modified substantially because it is added in large excess and, additionally, this is the only species that absorbs radiation, it is possible to assume, for this particular experiment and in a first approximation, that the behavior of the reaction can be represented by a pseudo-first order kinetic expression. Then, in accordance with Fogler [38]:

$$Da = \frac{k^* V_R}{Q} \quad (31)$$

This number can be estimated experimentally, regardless of a precise kinetic representation, through the following approximate expression:

Table 3
Kinetic rate constants for DCAA and FA.

Parameter	Reference value	Reference pH
k_8 (M^{-1} s^{-1})	5.82×10^7 (i)	3.2–3.5
	9.20×10^7 (ii)	6.2
k_{12} (M^{-1} s^{-1})	1.30×10^8 (iii)	1
	1.30×10^8 (iv)	1
k_{13} (M^{-1} s^{-1})	3.20×10^9 (v)	6

(i) Taken from [24]; (ii) taken from [29]; (iii) and (v) taken from: [25]; (iv) taken from [39];

$$\mathrm{Da} = \frac{V_R/Q}{C_i^0/R_{i,MAX}} \tag{32}$$

In the case of FA the maximum reaction rate takes place at the beginning of the experimental run ($t = 0$). This gives as a result that Da = 0.0086. If just to corroborate, one wish to take the case of the DCAA oxidation, the maximum reaction rate occurs at $t = 10{,}800$ s, which renders a value of Da = 0.0025. Thus, there is no doubt that even the maximum possible value of the conversion per pass will be quite small.

Considering the species that gives the greatest Da, (that is, FA) it is possible to accept the approach mentioned earlier (the pseudo-first order kinetics). In this case, it is conceivable to evaluate a pseudo-first order kinetic constant for the same experiment.

Taking all the corresponding experimental data and resorting to a simple parameter estimation method, after proposing that:

$$R_{FA} = k^* C_{FA} \tag{33}$$

A value of $k^* = 0.0073$ s^{-1} is obtained. Using to this expression, a more exact value of Da = 0.016 is calculated for the conditions of maximum reaction rate. If it is accepted that the previous equation is fulfilled for FA in this selected run, then the maximum conversion per pass is:

$$X = 1 - \exp[-k^*(Q/V_R)] = 0.0159 \tag{34}$$

This result clearly ratifies that the reactor operates under differential conversion.

If the conversion per pass is differential and the reactor has a system of fluid inlet, fluid outlet and mixing as described in Section 2.2, there are no possibilities for the existence of mass transfer control in the obtained kinetics. This situation was to be expected for the following reasons: (i) the reactor volume is very small, (ii) the recirculation flow rate is high, (iii) with the used concentrations and applied radiation rates, the reaction rate is slow and (iv) the design of the internal mixing as well as the special construction of the different parts of the reaction space generates high turbulence in the bulk of the fluid. Consequently, the resulting effect of all these factors is that the maximum conversion of the reagents per pass, even under the most unfavorable conditions, is extremely low.

Considering all these circumstances, added to the very small relationship between V_R/V_T guarantee the validity of the application of Eq. (1) and, even more important, for reactor design purposes, the intrinsic nature of the obtained kinetic rate equations.

4.2. Model evaluation for DCAA and FA separately

Table 3 shows a summary of the kinetic rate constants for FA_H, FA_A and DCAA for reaction with ·OH obtained from different works.

The ·OH radical rate constants for FA_H and FA_A forms are well known and have been extensively used in kinetic modeling of ·OH radical induced degradation of FA [33].

In the case of DCAA two kinetic rate constants were evaluated: (i) $k_8 = 5.8 \times 10^7$ M^{-1} s^{-1} reported in Zalazar et al. [24] at the same pH (3.5) as the current work and the rate constant determined by Maruthamuthu et al. [29] through a competition kinetics method against SCN^- at pH 6.2, a widely used probe in radiolysis: (ii) $k_8 = 9.2 \times 10^7$ M^{-1} s^{-1}.

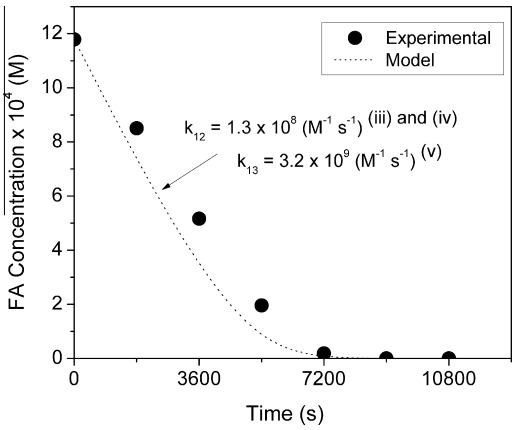

Fig. 2. Simulation results employing the rate constants adopted from the literature and included in the kinetic model, compared with the experimental values obtained in this work. (iii and v): values taken from Buxton et al. [25], (iv): values taken from Adams et al. [39].

Both values have the same order of magnitude. However the difference is important: 37%. This difference could be explained by the methods used in each case. Although the competition kinetic is a most appropriate method, the rate constant obtained in Zalazar et al. [24] is based on a model that provides a complete mechanism of the DCAA reaction. Therefore it is important to evaluate both constants with the proposed model to establish which one gives the best representation of the experimental data.

The system of ordinary differential equations [Eqs. (28)–(30)] was solved for each individual compound by taking the concentration of the other compound equal to zero. The estimations obtained were compared with the experiments conducted for each pollutant alone, i.e., a degradation experiment with FA alone and another with DCAA alone.

The predictions of the model and the experimental values for an experiment employing FA alone are shown in Fig. 2. The comparison shows that the model (solved with the adopted rate constants) represents the experimental data reasonably well.

For DCAA, the two values of the constants cited above were evaluated. The simulation results show that the calculated constant (i) represents the experimental data at pH = 3.5 much better (Fig. 3) than the constant obtained by Maruthamuthu et al. [29]. For this reason, the kinetic constant obtained by Zalazar et al. [24] was chosen for represent the degradation mixture of DCAA and FA.

If these values of the rate constants are considered correct, it is clear that the decomposition rate of FA is one order of magnitude larger than the one corresponding to DCAA. Thus, it should be expected that all the FA will be fully decomposed before the DCAA reaches an equivalent level of degradation.

4.3. Model evaluation for the mixture of DCAA and FA

The full set of experimental data described in Table 1 for each variable involved in the reaction was used to evaluate the quality of the mathematical model (represented by the system of ordinary differential equations derived before Eqs. (28)–(30)). This means that not only changes in the DCAA, FA and HP concentrations were studied, but also, variations in the irradiation rate conditions with lamps of different output power were considered. In accordance with the discussion of the previous section, the values of α and β

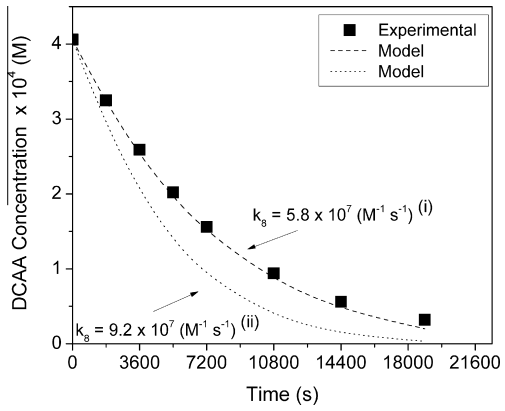

Fig. 3. Complementary experiments to confirm the adoption of the value of constant k_8. Simulation results with the rate constants adopted in this work compared with the experimental values. (i) Zalazar et al. [24], (ii) Maruthamuthu et al. [29].

were set using the data shown in Table 3, which were taken from the work of Zalazar et al. [24] and Buxton et al. [25].

The comparison between the model corresponding to the mixture and the experimental data for different irradiation levels (40 W and 15 W) and for three initial molar ratios defined as $r' = C^0_{H_2O_2}/C^0_{TOC}$ is presented in Fig. 4. In this definition, C_{TOC} is the total organic carbon (TOC) concentration corresponding to the mixture of both species (DCAA and FA).

In general, the simple model proposed was able to describe rather satisfactorily the experimental results. In addition, it predicts quite acceptably the concentration evolution of DCAA, FA, and HP for the two different irradiation levels used in this study. The major exception could be the case of FA.

It is seen that DCAA and FA decompositions increase with the molar ratio. However, these improvements leveled off for hydrogen peroxide dosages above 1.5×10^{-2} M (510 mg L^{-1}) at higher molar ratios due to the hydroxyl scavenging effect caused by the excess of hydrogen peroxide in water solutions. This optimum value of r' was experimentally found in a previous work [18]. For DCAA, employing the 40 W input power lamp, the range of values of r' between 2 and 6 ($C^0_{H_2O_2} = 3.9 \times 10^{-3} - 1.2 \times 10^{-2} M = 132 - 408$ mg L^{-1}) is the optimum to produce the highest conversions. For FA, the best operating conditions were found with values of r' between 2 and 8 ($C^0_{H_2O_2} = 3.9 \times 10^{-3} - 1.6 \times 10^{-2}$ M $= 132 - 544$ mg L^{-1}). A significant degradation of DCAA was only obtained with the 40 W irradiation power and with concentrations of hydrogen peroxide lower than 3.4×10^{-3} M (115 mg L^{-1}).

Fig. 4b and c provide a very practical outcome for different initial molar ratios. There is no sense to work over the whole range of technical feasible HP initial concentrations. On the contrary, the increase of H_2O_2 concentration more than the minimum necessary produces two adverse effects: (i) DCAA degradation is poorer and (ii) the excess of HP becomes very large, which conspires against the overall economy of the process. An initial concentration of hydrogen peroxide not larger than 3.4×10^{-3} M ($\sim$115 mg L^{-1}) is enough to decompose the mixture of both reactants.

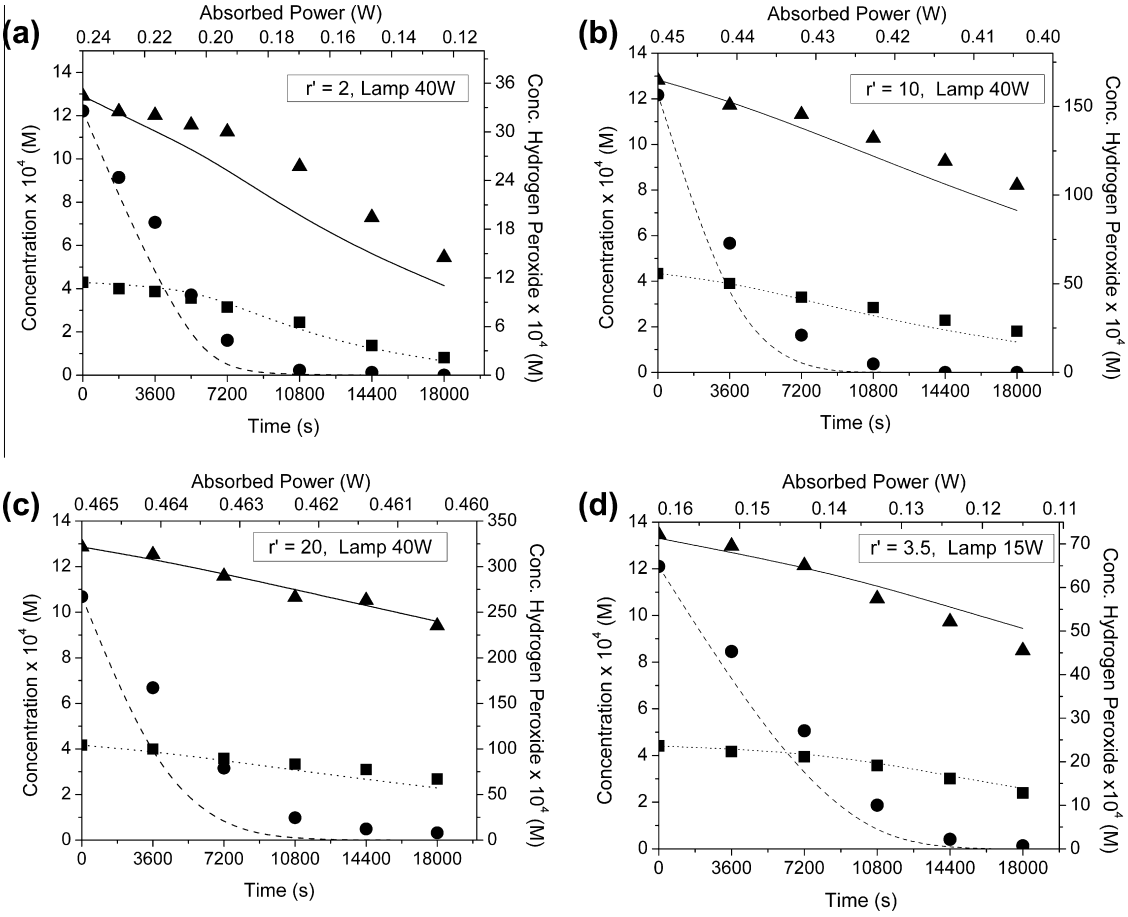

Fig. 4. Concentration evolution of simulation vs. experimental values as a function of time for: (■) C_{DCAA} experimental, (...) C_{DCAA} model; (●) C_{FA} experimental, (----) C_{FA} model and (▲) C_{HP} experimental, (—) C_{HP} model. (a) $C^0_{HP} = 9.7 \times 10^{-4}$ M; (b) $C^0_{HP} = 3.4 \times 10^{-3}$ M; (c) $C^0_{HP} = 3.2 \times 10^{-2}$ M; (d) $C^0_{HP} = 7.2 \times 10^{-3}$ M.

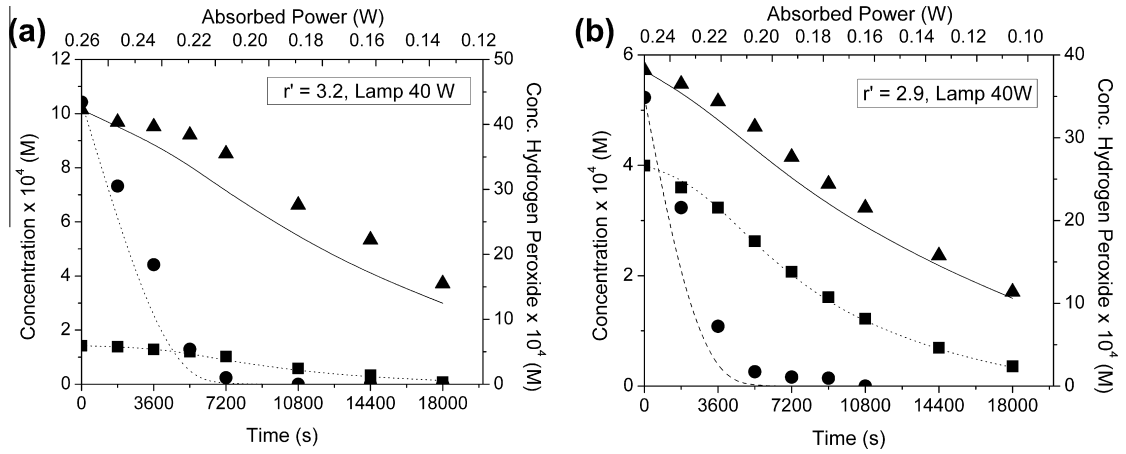

Fig. 5. Simulations vs. experimental values as a function of time for (■) C_{DCAA} experimental (...) C_{DCAA} model; (●) C_{FA} experimental, (----) C_{FA} model and (▲) C_{HP} experimental, (—) C_{HP} model. (a) $C^0_{DCAA} = 1.4 \times 10^{-4}$M; $C^0_{FA} = 1.1 \times 10^{-3}$M; $C^0_{HP} = 4.2 \times 10^{-3}$ M. (b) $C^0_{DCAA} = 3.9 \times 10^{-4}M$; $C^0_{FA} = 5.2 \times 10^{-4}$M; $C^0_{HP} = 3.8 \times 10^{-3}$ M.

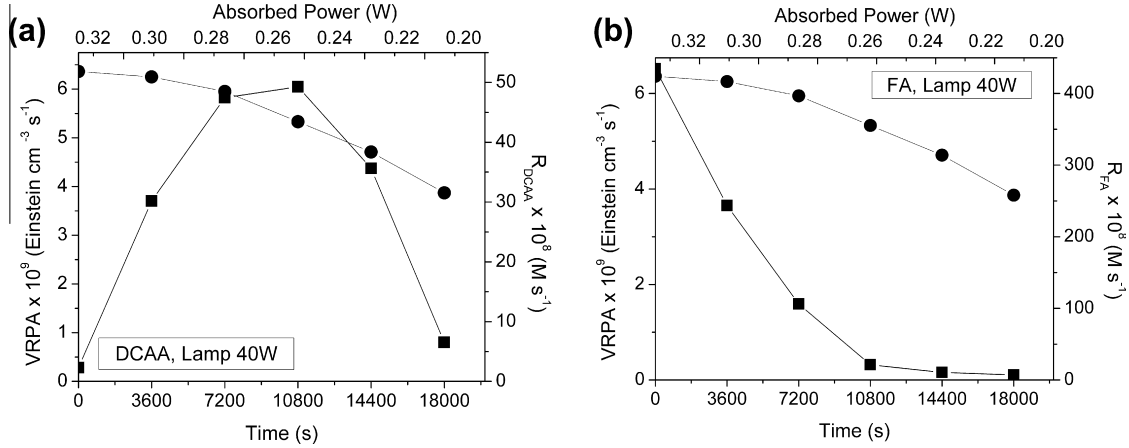

Fig. 6. (a) VRPA and reaction rate of DCAA disappearance values as a function of time (b) VRPA and reaction rate of FA disappearance values as a function of time. (■) Reaction Rate (●) VRPA.

In all figures we show the absorbed power (W) (top x-axis) used to degrade the parent compounds. These values were calculated according to the LVRPA × V_R values and converted into the corresponding W units for monochromatic radiation.

Fig. 5 shows the experimental and predicted values for different reactant's initial concentrations.

Note that the DCAA decay rate is lower at the beginning and it increases afterwards, when the concentration of FA becomes very low ($\sim 1 \times 10^{-4}$ M = 5 mg L^{-1}). Degradation of FA does not present this type of behavior.

These results indicate that during the first stages of the reaction, FA is preferentially degraded. DCAA anion reactivity toward the ·OH radical (strong electrophile) is much lower than that of the FA anion due to, on one-hand, the electron-withdrawing character of the two chlorine atom substituents in the –CH(Cl_2) moiety, which makes the H-atom less prone to abstraction by the ·OH radical, and on the other hand, the stereochemistry of the same moiety, which makes the H-atom less accessible to the ·OH radical attack.

This is in agreement with the values of the rate constants reported for FA and DCAA in Table 3.

To validate the different behaviors of DCAA and FA, the reaction rates of these compounds are represented in Fig. 6. This plot shows experimental values of the reaction rates of DCAA disappearance (R_{DCAA}) and the values of volume averaged LVRPA [$\langle \text{LVRPA}(x,t) \rangle_{V_R} = \text{VRPA}(t)$] for different reaction times and for a molar concentration ratio ($r' = C^0_{H_2O_2}/C^0_{TOC}$) equal to 3.1 (Fig. 6a). The same results are shown in Fig. 6b for FA. This type of results cannot be observed if a rigorous radiation model is not incorporated as a part of the kinetic model.

The variation in the VRPA is the result of the decrease in the HP concentration, which is the only compound that has significant radiation absorption at 253.7 nm. FA has a monotonous rate decrease because its reactivity, with respect to the hydroxyl radical, is higher. Also the reaction evolution of FA does not seem to show a strong competition with DCAA during the first stage of the process. Conversely, Fig. 6a is a clear representation of the way that this competition for the hydroxyl radicals affects the DCAA degradation. Reaction rates for DCAA reaches a maximum, which indicates that at the beginning of the reaction progress ·OH radicals attack FA preferentially; i.e., the compound that degrades faster. Only after about 2 h of reaction, DCAA seems to reach an equivalent efficiency in the capture of hydroxyl radicals. Thus, DCAA decomposition rate goes to a maximum and afterwards, as expected in a conventional performance, it decreases because both hydrogen peroxide and the DCAA concentrations decline.

The quality of the model may also be judged by comparing all experimental data (under different operating conditions) with the values obtained from model simulations. This can be seen in the "parity plot" for DCAA, FA, HP and chloride concentrations shown in Fig. 7.

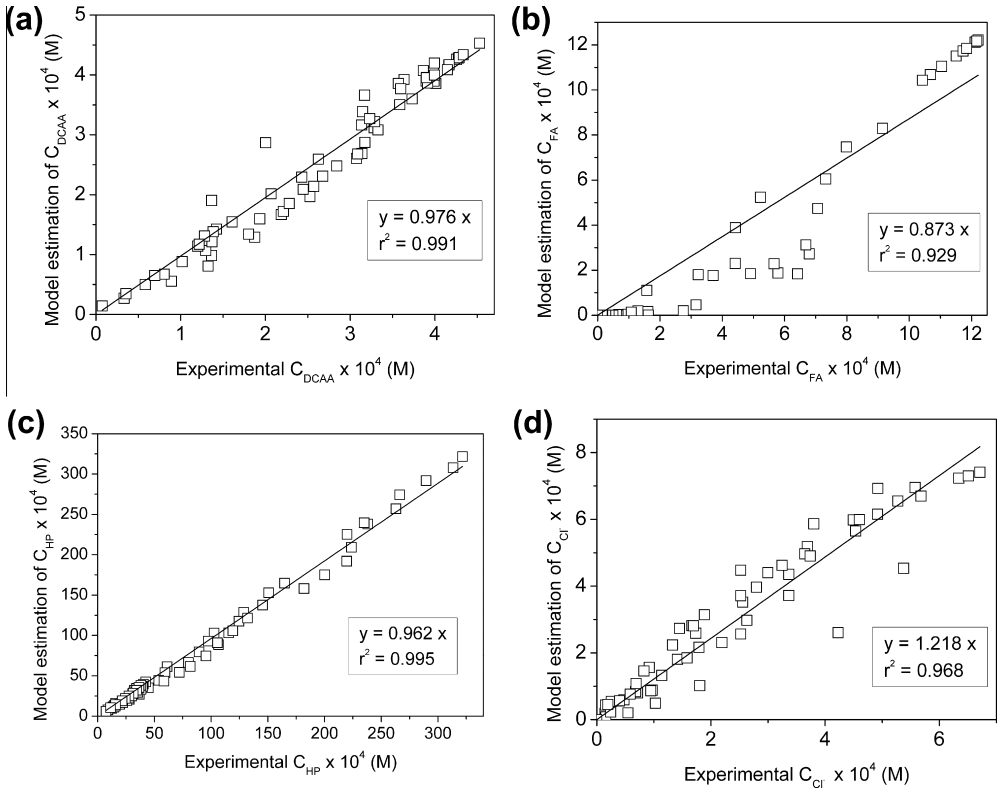

Fig. 7. (a) Simulated DCAA concentration vs. experimental values. (b) Simulated FA concentration vs. experimental values. (c) Simulated H_2O_2 concentration vs. experimental values. (d) Simulated Cl^- concentration vs. experimental values.

The distribution of the data around the "parity line" is a measure of the goodness of the model. In the case of DCAA and HP the simulations obtained with the model results agree with the experimental values. However, the comparison between the experimental and predicted concentrations of FA showed less agreement in the area corresponding to medium concentrations but the points are distributed almost evenly on both sides of the straight line. For the case of chloride, the points are a little more scattered around the parity line but also they are distributed almost evenly on both sides of the straight line. The plots also show the values corresponding to r^2 for the lines depicted in the plots. These values provide an additional confirmation of the accuracy of the mathematical model.

These figures show that the model for the mixture, which is simple and uses the mechanistic sequence of the decomposition of both compounds obtained separately, can be used to predict the degradation of the mixture, although both compounds have significant differences in their chemical reactivity.

This work was carried out with a mixture of different chemical compounds in pure water. In practical applications there are at least two additional factors that should be taken into account: (1) Real waters may have a different pH and (2), by the same token, the presence of organic matter, such as humic acids or some inorganic salts, or more specifically different carbonates and bicarbonates, can produce important changes in the reaction environment. It must be also considered that the proposed methodology may have several limitations and some complications that can be encountered in this type of situations.

Finally, is it can also be important to mention that the UV/H_2O_2 process is a powerful oxidant technology and, due to its very high reactivity, any possible remains of organic matter existing in the water streams should have been decomposed after the process. It would minimize the possibility of production of undesired by-products in the distribution system.

5. Conclusions

A simplified, but acceptably accurate, kinetic model has been developed for the degradation of the mixture of DCAA and FA employing UV radiation and H_2O_2. The reactor model includes the effect of radiation absorption on the reaction rates. Simulations results of concentrations evolutions of DCAA, FA, H_2O_2 and HCl from the model are in reasonable agreement with experimental data.

By applying this methodology, it is possible to progress from simple mixtures to more complex compositions. But at the same time, as systems are becoming more intricate and also incorporate the effects of other components that are usually present in water courses, the main challenge will be to prove that, perhaps with some modifications, this approach will still be able to describe all the new variables that affect the kinetics of the oxidation processes.

Acknowledgements

The authors would like to thank to Universidad Nacional del Litoral, Consejo Nacional de Investigaciones Científicas (CONICET) and Agencia Nacional de Promoción Científica y Tecnológica for their financial support. Also to Bárbara Cassano and Margarita Herman for the English language editing.

References

[1] H.D. Burrows, M. Canle, J.A. Santaballa, S. Steenken, Reaction pathways and mechanisms of photodegradation of pesticides, J. Photochem. Photobiol., B 67 (2002) 71–108.
[2] P. Gogate, A. Pandit, A review of imperative technologies for wastewater treatment II: hybrid methods, Adv. Environ. Res. 8 (2004) 553–597.

[3] K. Ikehata, M. Gamal El-Din, Aqueous pesticide degradation by hydrogen peroxide/ultraviolet irradiation and Fenton-type advanced oxidation processes: a review, J. Environ. Eng. Sci. 5 (2006) 81–135.
[4] O. Alfano, R. Brandi, A. Cassano, Degradation kinetics of 2,4-D in water employing hydrogen peroxide and UV radiation, Chem. Eng. J. 82 (2001) 209–218.
[5] Q. Hu, C. Zhang, Z. Wang, Y. Chen, K. Mao, X. Zhang, Y. Xiong, M. Zhu, Photodegradation of methyl tert-butyl ether (MTBE) by UV/H_2O_2 and UV/TiO_2, J. Hazard. Mater. 154 (2008) 795–803.
[6] M. Hügul, R. Apak, S. Demirci, Modeling the kinetics of UV/hydrogen peroxide oxidation of some mono-, di-, and trichlorophenols, J. Hazard. Mater. B 77 (2000) 193–208.
[7] H.Y. Shu, M.C. Chang, W.P. Hsieh, Remedy of dye manufacturing process effluent by UV/H_2O_2 process, J. Hazard. Mater. 128 (2006) 60–66.
[8] M.L. Marechal, Y.M. Slokar, T. Taufer, Decoloration of chlorotriazine reactive azo dyes with H_2O_2/UV, Dyes Pigm. 33 (1997) 281–298.
[9] F.S. García Einschlag, C. Luciano, A.L. Capparelli, Competition kinetics using the UV/H_2O_2 process: a structure reactivity correlation for the rate constants of hydroxyl radicals toward nitroaromatic compounds, Chemosphere 53 (2003) 1–7.
[10] O.M. Alfano, A. E. Cassano, Scaling-up of photoreactors applications to advanced oxidation processes, in: H. De Lasa, B. Serrano-Rosales (Eds.), Advances in Chemical Engineering, vol. 36, Photocatalytic Technologies, Elsevier, ISBN: 978-0-12-374763-1, 2009, pp. 229–287.
[11] Y.S. Lay, Oxidation of 1,2-dibromo-3-chloropropane in groundwater using advanced oxidation processes, 1989, Ph.D. dissertation, University of California, Los Angeles.
[12] W. Glaze, Y. Lay, J. Kang, Advanced oxidation processes. A kinetic model for the oxidation of 1,2-dibromo-3-chloropropane in water by the combination of hydrogen peroxide and UV radiation, Ind. Eng. Chem. Res. 34 (1995) 2314–2323.
[13] C. Liao, M. Gurol, Chemical oxidation by photolytic decomposition of hydrogen peroxide, Environ. Sci. Technol. 29 (1995) 3007–3014.
[14] M.I. Stefan, A.R. Hoy, J.R. Bolton, Kinetics and mechanism of the degradation and mineralization of acetone in dilute aqueous solution sensitized by the UV photolysis of hydrogen peroxide, Environ. Sci. Technol. 30 (1996) 2382–2390.
[15] J.C. Crittenden, H. Shumin, D.W. Hand, S.A. Green, A kinetic model for H_2O_2/UV process in a completely mixed batch reactor, Water Res. 33 (1999) 2315–2328.
[16] W. Song, V. Ravindran, M. Pirbasari, Process optimization using a kinetic model for the ultraviolet radiation-hydrogen peroxide decomposition of natural and synthetic organic compounds in groundwater, Chem. Eng. Sci. 63 (2008) 3249–3270.
[17] H. Kusic, D. Juretic, N. Koprivanac, V. Marin, A. Loncaric Bonzic, Photooxidation processes for an azo dye in aqueous media: modeling of degradation kinetic and ecological parameters evaluation, J. Hazard. Mater. 185 (2011) 1558–1568.
[18] M. Mariani, M. Labas, R. Brandi, A. Cassano, C. Zalazar, Degradation of a mixture of pollutants in water using the UV/H_2O_2 process, Water Sci. Technol. 61 (2010) 3026–3031.
[19] C. Zalazar, M. Labas, R. Brandi, A. Cassano, Dichloroacetic acid degradation employing hydrogen peroxide and UV radiation, Chemosphere 66 (2007) 808–815.
[20] S. Murov, I. Carmichael, G. Hug, Handbook of Photochemistry, second ed., Marcel Dekker, New York, 1993.
[21] C. Zalazar, M. Labas, C. Martín, R. Brandi, O. Alfano, A. Cassano, The extended use of actinometry in the interpretation of photochemical reaction engineering data, Chem. Eng. J. 109 (2005) 67–81.
[22] A. Allen, C. Hochanadel, J. Ghormley, T. Davis, Decomposition of water and aqueous solutions under mixed fast neutron and gamma radiation, J. Phys. Chem. 56 (1952) 575–586.
[23] A.E. Cassano, O.M. Alfano, Reaction engineering of suspended solid heterogeneous photocatalytic reactors, Catal. Today 58 (2000) 167–197.
[24] C. Zalazar, M. Lovato, M. Labas, R. Brandi, A. Cassano, Intrinsic kinetics of the oxidative reaction of dichloroacetic acid employing hydrogen peroxide and ultraviolet radiation, Chem. Eng. Sci. 62 (2007) 5840–5853.
[25] G. Buxton, C. Greenstock, W. Helman, A. Ross, Critical review of data constants for reactions of hydrated electrons, hydrogen atoms and hydroxyl radicals in aqueous solutions, J. Phys. Chem. Ref. Data 17 (1988) 513–886.
[26] W. Koppenol, J. Butler, J. Van Leeuwen, The Haber–Weiss cycle, Photochem. Photobiol. 28 (1978) 655–660.
[27] K. Schested, O. Rasmussen, H. Fricke, Rate constants of OH with HO_2, O_2^- and $H_2O_2^+$ from hydrogen peroxide formation in pulse-irradiated oxygenated water, J. Phys. Chem. 72 (1968) 626–631.
[28] Beck, Detection of charged intermediate of pulse radiolysis by electrical conductivity measurements, Int. J. Radiat. Phys. Chem. 1 (1969) 361–371.
[29] P. Maruthamuthu, S. Padmaja, R. Huie, Rate constants for some reactions of free radicals with haloacetates in aqueous solution, Int. J. Chem. Kinet. 27 (1995) 605–612.
[30] R. Mertens, C. von Sonntag, J. Lind, G. Merenyi, A kinetic study of the hydrolysis of phosgene in aqueous solution by pulse radiolysis, Angew. Chem. Int. Ed. Engl. 33 (1994) 1259–1261.
[31] P. Neta, R. Huie, A. Ross, Rate constants for reactions of inorganic radicals in aqueous solution, J. Phys. Chem. Ref. Data 17 (1988) 1027.
[32] C. Zalazar, R. Romero, C. Martín, A. Cassano, Photocatalytic intrinsic reaction kinetics: I. Mineralization of dicholoroacetic acid, Chem. Eng. Sci. 60 (2005) 5240–5254.
[33] G. Imoberdorf, M. Mohseni, Modeling and experimental evaluation of vacuum – UV photoreactors for water treatment, Chem. Eng. Sci. 66 (2011) 1159–1167.
[34] J. Krýsa, G. Waldner, H. Mest ánková, J. Jirkovský, G. Grabner, Photocatalytic degradation of model organic pollutants on an immobilized particulate TiO_2 layer. Roles of adsorption processes and mechanistic complexity, Appl. Catal. B 64 (2006) 290–301.
[35] M. Dijkstra, H. Panneman, J. Winkelman, J. Kelly, A. Beenackers, Modeling the photocatalytic degradation of formic acid in a reactor with immobilized catalyst, Chem. Eng. Sci. 57 (2002) 4895–4907.
[36] J.H. Baxendale, J.A. Wilson, Photolysis of hydrogen peroxide at high light intensities, Trans. Faraday Soc. 53 (1957) 344–356.
[37] D.H. Volman, J.C. Chen, The photochemical decomposition of hydrogen peroxide in aqueous solutions of allyl alcohol at 2537 Angstroms, J. Am. Chem. Soc. 81 (16) (1959) 4141–4144.
[38] H.S. Fogler, Elements of Chemical Reaction Engineering, fourth ed., Prentice Hall Int, New York, 2006.
[39] G.E. Adams, J.W. Boag, J. Currant, B.D. Michael, Absolute rate constants for the reaction of the hydroxyl radical with organic compounds, in: M. Ebert, J.P. Keene, A.J. Swallow, J.H. Baxendale (Eds.), Pulse Radiolysis, Academic Press, New York, 1965, pp. 131–143